http://dx.doi.org/10.5012/bkcs.2012.33.3.763

Articles

Unusual Non-magnetic Metallic State in Narrow Silicon Carbon Nanoribbons by Electron or Hole Doping†

Ping Lou[‡,§,*] and Jin Yong Lee[‡,#,*]

[‡]*Department of Chemistry, Sungkyunkwan University, Suwon 440-746, Korea.* [*]*E-mail: jinylee@skku.edu*
[§]*Department of Physics, Anhui University, Hefei 230039, Anhui, P.R. China.* [*]*E-mail: loup@ahu.edu.cn*
[#]*Supercomputing Center, Korea Institute of Science and Technology Information, Yuseong, Daejeon 305-806, Korea*
Received May 18, 2011, Accepted August 31, 2011

We investigated the width (*N*) dependence on the magnetization of *N*-ZSiC NR with electron and hole doping on the basis of systematic DFT calculations. The critical values of the upper and down critical concentration to give the maximum and zero magnetic moment at edge Si/C atoms by electron/hole doping ($x_{up,e}$, $x_{down,e}$, $x_{up,h}$, and $x_{down,h}$) depend on the width of *N*-ZSiC NR. Moreover, due to $x_{up,e} \neq x_{up,h}$ and $x_{down,e} \neq x_{down,h}$, the electron and hole doping effect are asymmetry, i.e, the critical electron doping value ($x_{down,e}$) is smaller than the critical hole doping value ($x_{down,h}$) and is almost independent of the width of *N*ZSiC NR though the other critical values of the electron and hole doping that influence the magnetization of *N*-ZSiC NR depend on the width. It was also found that at $x_{down,e}$ or $x_{down,h}$ doping, the *N*-ZSiC NR turns into *unusual non-magnetic metallic* state. The magnetic behavior was discussed based on the band structures and projected density of states (PDOS) under the effect of electron/hole doping.

Key Words : Magnetic, Silicon carbon nanoribbon, Electron doping, Hole doping, Band structure

Introduction

Spintronic devices are believed to be smaller, faster, and far more versatile than the conventional electronic devices, which have the following functioning scheme: (1) information is stored (written) into spins as a particular spin orientation (up or down), i.e., the *magnetization*, (2) the spins, being attached to mobile electrons, carry the information along a wire, i.e., the *spin-polarized electron transport*, and (3) the information is read at a terminal. The key feature is the control and manipulation of the 'spin' of the electron, instead of its charge that is the focus of the electronics.[1] It is noted that the graphene nanoribbons (NRs) offer a possibility of achieving these purposes.[2-7] Hence, the graphene NRs have attracted a lot of interest.[8-45] The graphene NRs are made by cutting the graphene sheets, where the edge carbon atoms are passivated by hydrogen. It was found that the graphene NRs can be either metallic or semiconducting depending on the width and structure of the edges.[8-18] Notably, the zigzag graphene NRs (graphene nanoribbons with zigzag edges) are a magnetic semiconductor with a small band gap, and have ferromagnetic ordering at each edges and their spins at two opposite edges are antiparallel.[16,19-28] When a very strong transverse electric field is applied, the ZG NRs transform to half metal,[19-22] where only one of the spin channels conducts and the other remains insulating, which suggests possibility for the control and manipulation of the *spin-polarized electron transport* by applying electric field.

However, an easy way to control the spin polarized electrons in downscaling devices has proved to be quite a challenge. It has proven elusive to manipulate the *magnetization* by applying electric field.[46,47] We recently reported that the zigzag silicon carbon nanoribbons (ZSiC NRs) can be utilized for manipulating the *magnetization* by applying an electric field[48] and carrier (hole and electron) doping.[49] It was found that the ZSiC NRs showed the *magnetization* by a transverse electric field as well as the conversion of spin polarization.[48] It was also found that holes and electrons injected by removing or adding electrons from the ZSiC NRs resulted in the magnetization and change of the magnetization direction of the ZSiC NRs.[49] Here, we present new findings on the *N*-ZSiC NR by hole and electron doping. We investigated the width (*N*) dependence on the magnetization of *N*-ZSiC NR with electron and hole doping. In particular, electron and hole doping resulted in asymmetric effect. The most important finding is that, at the critical electron doping or the critical hole doping, the *N*-ZSiC NR starts to turn into a *strange non-magnetic metalic* state. In case when the electron doping leads to the *N*-ZSiC NR's *non-magnetic metalic* state, the edge Si forms conduction, while the edge C forms insulation. On the contrary, when the hole doping leads to the *N*-ZSiC NR's *non-*

†This paper is to commemorate Professor Kook Joe Shin's honourable retirement.

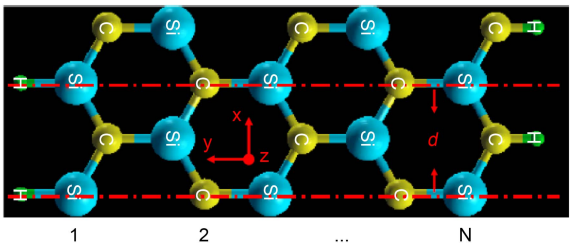

Figure 1. (color online) Geometric structure of the *N*-ZSiC NR. ZSiC NR is periodic along the *x* direction. The 1D unit cell distance and the ribbon width are denoted by *d* and *N*, respectively. The large, middle, and small spheres denote Si, C, and H atoms, respectively.

magnetic metalic state, the edge C forms conduction, while the edge Si forms insulation.

Models and Methods

In our model, *N*-ZSiC NRs is flat in *x*-*y* plan, with *N*-zigzag chains along *x* direction. The edges of ZSiC NRs are saturated by hydrogen atoms. Periodic boundary condition (PBC) is used to consider ZSiC NRs with infinite length, which is shown in Figure 1. Our calculations were carried out with the OPENMX computer code.[50] The DFT within the GGA[51] for the exchangecorrelation energy was adopted. Norm-conserving Kleinman-Bylander pseudopotentials[52] were employed, and the wave functions were expanded by a linear combination of multiple pseudo atomic orbitals (LCPAO)[53,54] with a kinetic energy cutoff of 250 Ry. The basis functions used were: C6.0-s2p2d1, Si6.0-s2p2d1, and H4.5-s1p1. The first symbol designates the chemical name, followed by the cutoff radius (in Bohr radius) in the confinement scheme and the last set of symbols defines the primitive orbitals applied. We adopted a supercell geometry (Figure 1) where the length of a vacuum region along the non-periodic direction (*y*-, *z*-directions) was 20 Å, and the lattice constant along the periodic direction (*x*-direction) was 3.11 Å. Previously, it was suggested that the enough number of *k*-point sampling in the Brillouin zone integration should be performed for reliable results.[55,56] Thus, we used 120 × 1 × 1 *k*-point sampling points in the Brillouin zone integration. The geometries were optimized until the Hellmann-Feynman forces were less than 10^{-4} Hartree/bohr. The convergence in energy was 10^{-8} Hartree. We have also increased the size of the supercell to make sure that it does not produce any discernible difference on the results. Holes and electrons doping were performed by a shift in the Fermi level and a uniform background charge is introduced to balance the charge neutrality of the system, which is called as the Fermilevel shift (FLS) method.

Results and Discussion

Figure 2 shows the magnetic moments of the total unit cell and at the edge Si and C of *N*-ZSiC NRs in the ground state as a function of the doping concentration *x* per unit cell. In

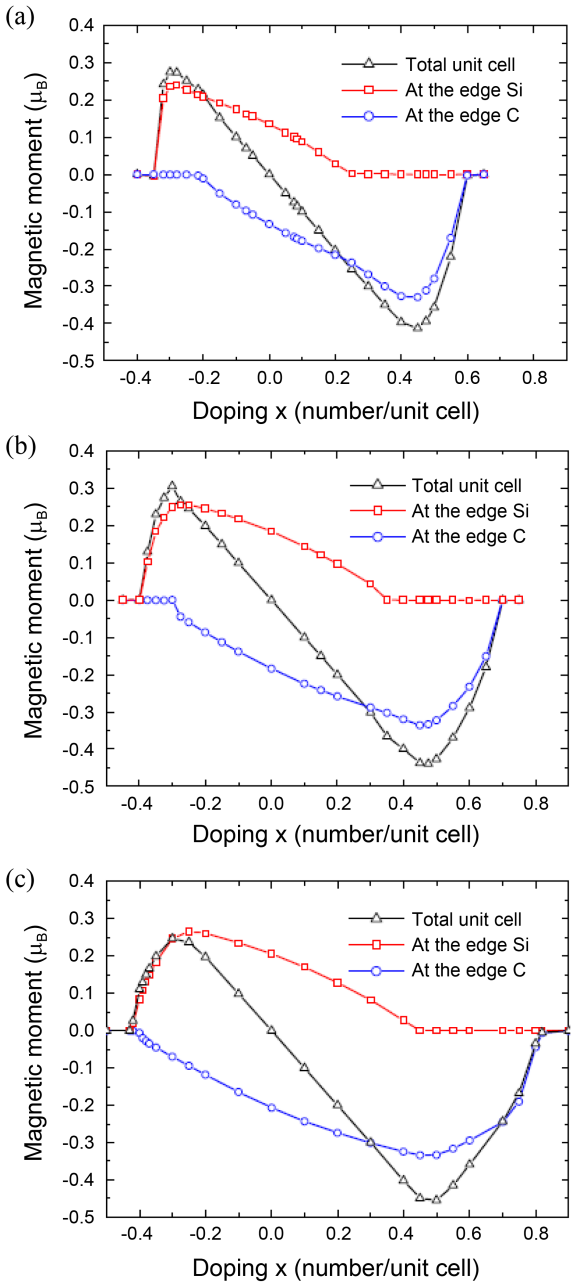

Figure 2. (color online) Magnetic moments of the total unit cell and at the edge Si and C of *N*-ZSiC NRs for (a) $N = 4$, (b) $N = 6$, and (c) $N = 8$ in the ground state as a function of the doping concentration *x* per unit cell ($x = 0$ for un-doping, $x < 0$ for electron doping, and $x > 0$ for hole doping).

our previous study, it was known that when the hole is doped, the local magnetic moment at the edge C atoms is enhanced, while the local magnetic moment at the edge Si atoms is weakened, hence the ZSiC NR has been *magnetized* by hole doping. It is noted that the magnetization direction is spin-down, and the total magnetic moment conforms to the local magnetic moment at the edge C atoms. The opposite trend appears by electron doping. It should be noted that the critical values of $x_{up,e}$, $x_{down,e}$, $x_{up,h}$, and $x_{down,h}$ depend on the width of *N*-ZSiC NR. Here $x_{up,e}/x_{up,h}$ and $x_{down,e}/x_{down,h}$ denote the upper and down critical concentration of electron/hole

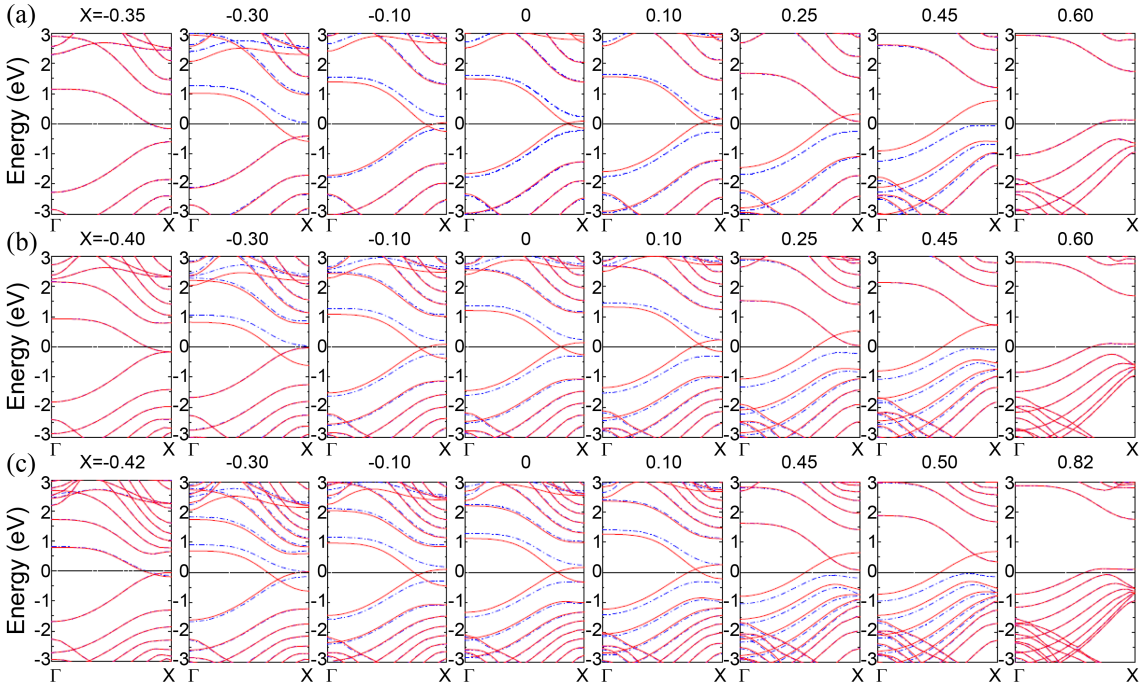

Figure 3. (color online) Band structures of *N*-ZSiC NRs for (a) $N = 4$, (b) $N = 6$, and (c) $N = 8$ in ground state as a function of the doping concentration x per unit cell. The red solid and blue dash-dotted lines denote the spin-up and spin down bands, respectively. The Fermi level is set to zero.

doping to give the maximum and zero magnetic moment at edge Si/C atoms, respectively. Moreover, due to $x_{up,e}$ $x_{up,h}$ and $x_{down,e}$ $x_{down,h}$, the electron and hole doping effect are asymmetry.

In order to further analyze the above results, in Figure 3 we show the band structures of *N*-ZSiC NRs ($N = 4$, 6, and 8) for $x = x_{up,e}$, $x_{down,e}$, $x_{up,h}$, and $x_{down,h}$ critical doping values as well as $x = -0.10$, 0.00, and 0.10. In general, as shown in Figure 3, without doping (x=0), the ZSiC NR is ferrimagnetic semiconductor with two different direct band gaps for the spin-up and the spin-down channels at near the X point.[55] For the electron doping ($x < 0$), due to the extra electron from the doping, the fermi level of the system is shifted upward and crosses the conduction band in the spin up channel, which indicates that the ZSiC NR turns into ferrimagnetic metal state. The spin-up and the spin-down channels of the valence band approach closer each other, which leads to the weakened local magnetic moment at the edge C, while the spin-up and the spin-down channels of the conduction band are more separated, which leads to the enhanced local magnetic moment at the edge Si. It is noted that when $x = x_{up,e}$, the spin-up and the spin-down channels of the valence band coincide each other, which leads to the zero local magnetic moment at the edge C, while the separation of the spin-up and the spin-down channels of the conduction band reaches the maximum, which leads to the maximum local magnetic moment at the edge Si as shown in Figure 3. The values of $x_{up,e}$ were calculated to be for –0.30, –0.30, and –0.30 for $N = 4$, 6, and 8, respectively. By further electron doping, when $x = x_{down,e}$, the spin-up and the spin-down channels of the conduction band are also coincide

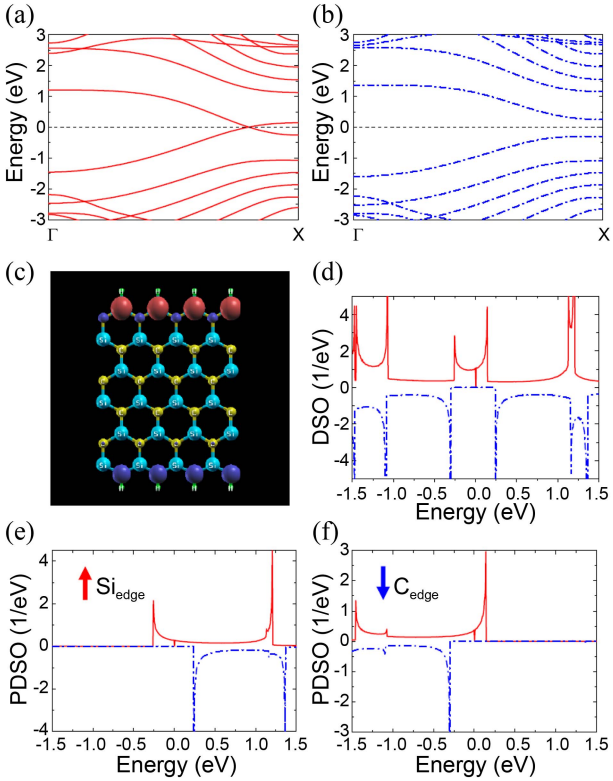

Figure 4. (color online) Band structures of 6-ZSiC NR for (a) the spin-up and (b) spin down bands, (c) spatial distribution of the spin differences, (d) total electronic density of states (DOS), and the projected DOS (PDOS) for (e) edge Si and (f) edge C atoms. The red solid and blue dash-dotted lines denote the spin-up and spin-down bands, respectively. The Fermi level is set to zero. The red and blue arrows denote the direction of the spin-up and spin-down at the edge atoms.

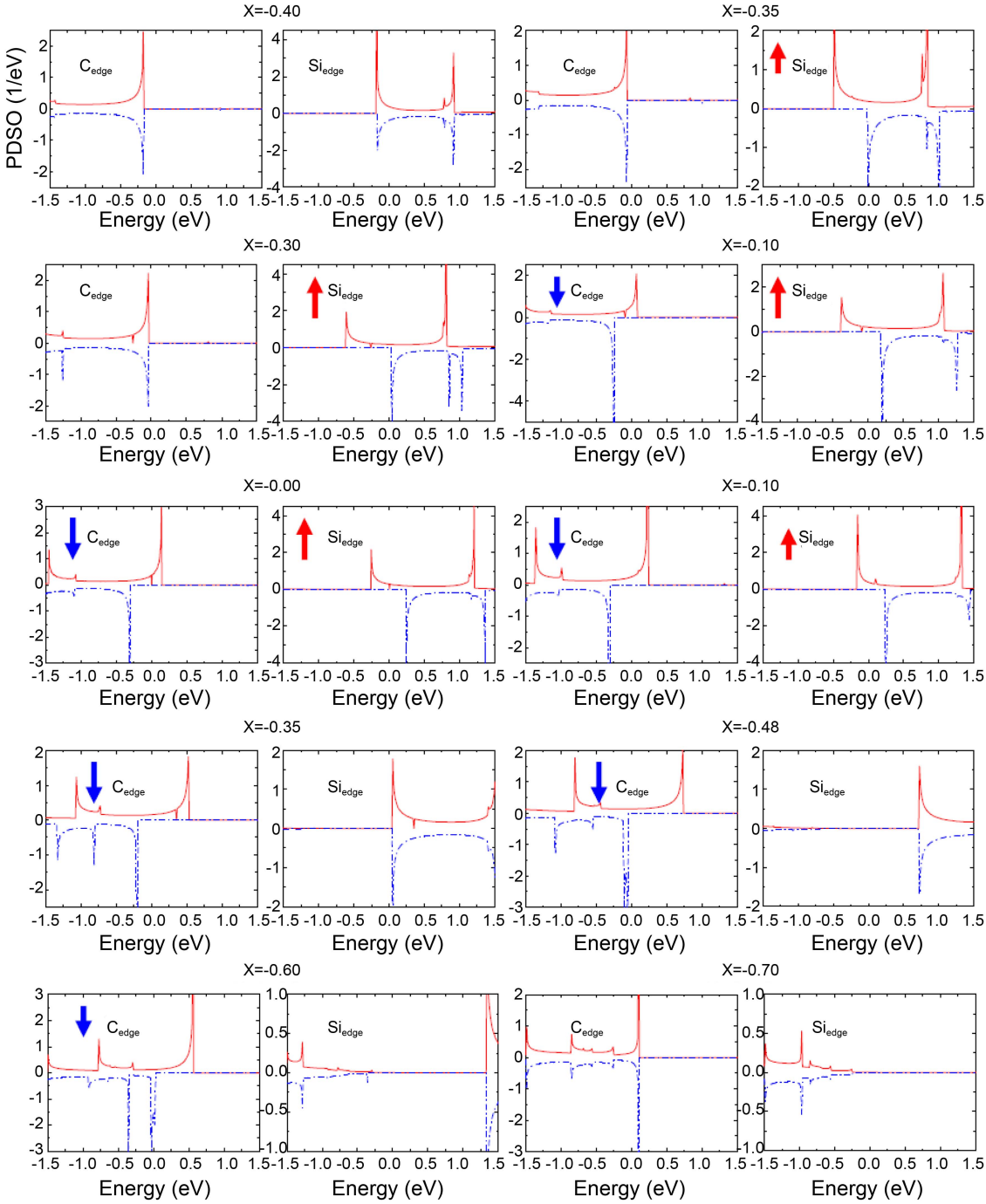

Figure 5. (color online) PDOS for the edge C and Si atoms of 6-ZSiC NR as a function of the doping concentration x per unit cell (x =0 for un-doping, $x < 0$ for electron doping, and $x > 0$ for hole doping). The Fermi level is set to zero. The other marks are same as in Figure 4.

each other, which leads to the zero local magnetic moment at the edge Si, and the ZSiC NR turns into a non-magnetic metal state. The values of $x_{down,e}$ were calculated to be −0.35, −0.40, and −0.42 for N = 4, 6, and 8, respectively. The opposite trend was obtained by hole doping as reported previously.[49] The values of $x_{up,h}/x_{down,h}$ were calculated to be 0.45/0.60, 0.48/0.70, and 0.50/0.82 for N = 4, 6, and 8, respectively.

Why the increased/decreased separation of the spin-up and the spin-down channels of the valence band leads to the enhanced/reduced local magnetic moment at the edge C, while the increased/decreased separation of the spin-up and the spin-down channels of the conduction band leads to the enhanced/reduced local magnetic moment at the edge Si? To answer these questions, we looked into the band structures, spatial distribution of the spin differences, total electronic density of states, and the projected local density of states (PDOS) of the edge Si and C for 6-ZSiC NR without doping. As seen in Figure 4(a) and (b), the valence and conduction bands for the spin-up and spin-down channels are close to

the Fermi level. For these bands, the electron spins are distributed over the edge Si and C atoms (Figure 4(c)), and thus PDOS of the edge Si and C may include all the information of the four bands including the local magnetic moment at the edge Si and C. Thus, we focused on PDOS for the edge Si and C atoms in different electron and hole doping condition.

Figure 5 shows PDOS for the edge C and Si atoms in 6-ZSiC NR for doping concentrations $x = -0.42$, -0.35, -0.30, -0.10, 0.00, 0.10, 0.35, 0.48, 0.60, and 0.70. Without doping ($x = 0$), PDOS shows that the spin-up and the spin-down channels of the edge C as well as the edge Si are well separated from the Fermi level indicating that the edge C and Si are spin-polarized. For the edge Si atoms, the spin-up channel shows the PDOS below the Fermi level, while the spin-down channel above the Fermi level. As a result, the edge Si atoms have spin-up local magnetic moment. Oppositely for the edge C atoms, the PDOS in the spin-down channel is below the Fermi level, while the spin-up channel above the Fermi level, resulting in the local magnetic moment of spin-down in the edge C atoms.

By a little electron doping, such as $x = -0.10$, due to the extra electron from the doping, the Fermi level of the system is shifted upward. Thus, for the edge Si atoms, the number of electrons in the spin-up channel in the valence band (below the Fermi level) increases, while the PDOS in the spin-down channel is still above the Fermi level. As a result, the net number of electrons with up spin increases and the local magnetic moment at the edge Si is enhanced. As for the edge C atoms, due to the upward shifted Fermi level, the area of PDOS in the spin-up channel below the Fermi level increases, i.e., the number of electrons in the spin-up channel increases. On the other hand, the PDOS in spin-down channel is still below the Fermi level. As a result, the local magnetic moment at the edge C is reduced. As electron doping increases, the Fermi level of the system is further shifted upward, thus, for the edge Si atoms, the local magnetic moment at the edge Si increases further. However, for the edge C atoms, as electron doping increases, the net number of electrons below the Fermi level in the spin-down decreases, which leads to the further reduction in the local magnetic moment at the edge C. When $x = -0.30$, the area of PDOS below the Fermi level in the spin-up channel of the edge Si atoms is the maximum, as a result, the local magnetic moment at the edge Si reaches the maximum. At same time, the areas of PDOSs below the Fermi level in the spin-up and spin-down channels of the edge C atoms are coincidently the same, which indicates that the local magnetic moment at the edge C disappears. After that, as electron doping increases further ($x = -0.35$), for the edge Si atoms, the area of PDOS below the Fermi level in the spin-up channel turns to decrease because the PDOS in the spin-up channel turns to move up, while the PDOS in the spin-down channel move down further and crosses with the Fermi level. As a result, the local magnetic moment at the edge Si turns to decrease. When $x = -0.40$, the areas of PDOSs below the Fermi level in the spin-up and spin-down channels of the edge Si atoms are coincidently the same, which leads to the local magnetic moment at the edge Si of zero, then, 6-ZSiC NR turns to be no more spin-polarized. On the other hand, since the PDOSs in the spin-up and spin-down channels of the edge Si atoms cross the Fermi level, 6-ZSiC NR turns into the *unusual non-magnetic metallic* state. Because the PDOSs in the spin-up and spin-down channels of the edge C atoms are below the Fermi level and do not cross the Fermi level, the edge C is insulator state.

In contrast, by a little hole doping, such as $x = 0.10$, due to the missing electron, the Fermi level of the system is shifted

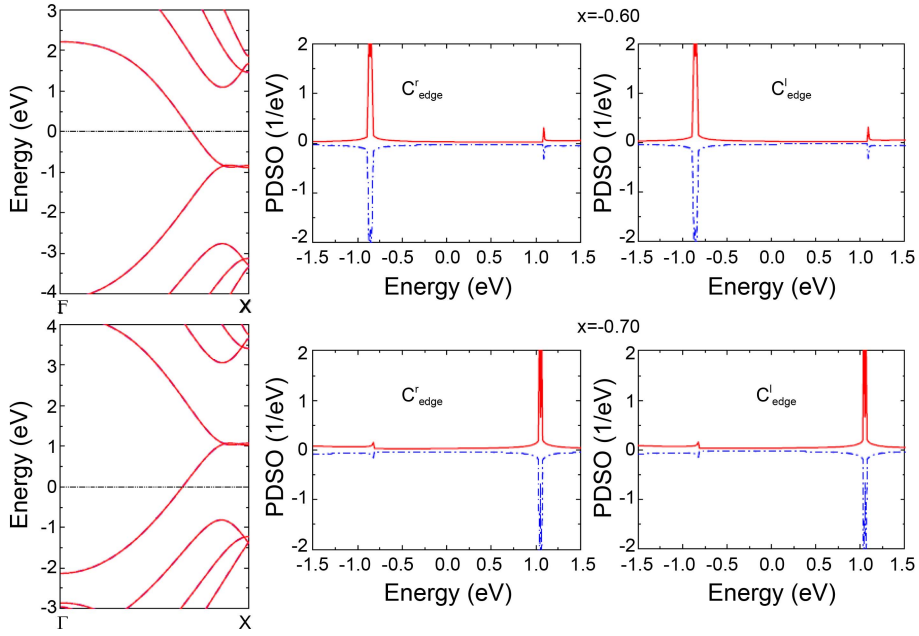

Figure 6. (color online) Band structure and PDOS of the right and left edge C atoms of 4-ZCNR for the (a) electron doping $x = -0.60$ and (b) hole doping $x = 0.70$. The Fermi level is set to zero, and the notation is the same as in Figure 4.

downward. Thus, for the edge C atoms, the area of PDOS below the Fermi level in the spin-up channel decreases. While the PDOS below the Fermi level in the spin-down channel is still below the Fermi level. As a result, the net number of electrons with down spin increases and the local magnetic moment at the edge C is enhanced. As for the edge Si atoms, due to the downward shifted Fermi level, the area of PDOS in the spin-up channel below the Fermi level decreases, i.e., the number of electrons in the spin-up channel decreases. On the other hand, the PDOS in spin-down channel is still above the Fermi level. As a result, the net number of electrons with spin-up decreases, hence the local magnetic moment at the edge Si is reduced. As hole doping increases, the Fermi level of the system is further shifted downward, thus, the local magnetic moment at the edge Si decreases further. However, for the edge C atoms, as hole doping increases, the net number of electrons below the Fermi level in the spin-down increases, which leads to the further enhancement in the local magnetic moment at the edge C. When $x = 0.35$, the areas of PDOS below the Fermi level in the spin-up and spin-down channels of the edge Si atoms are coincidently the same, as a result, the local magnetic moment at the edge Si disappears. As for the edge C atoms, due to the increase in net number of electrons below the Fermi level with spin-down, the local magnetic moment at the edge C increases further. When $x = 0.48$, the net number of electrons below the Fermi level in the spin-down channel of the edge C atoms is the maximum, as a result, the local magnetic moment at the edge C reaches the maximum. After that, as hole doping increases, for the edge C atoms, the area of PDOS below the Fermi level in the spin-up channel turns to increase because the PDOS in the spin-up channel shifted down, while the PDOS in the spin-down channel shifted up further and crosses the Fermi level. Consequently, the local magnetic moment at the edge C turns to decrease ($x = 0.60$). When $x = 0.70$, the areas of PDOS below the Fermi level in the spin-up and spin-down channels of the edge C atoms are coincidently the same, which leads to the local magnetic moment at the edge C of zero, then, 6-ZSiC NR turns to be no more spin-polarized. On the other hand, since the PDOSs in the spin-up and spin-down channels of the edge C atoms cross the Fermi level, 6-ZSiC NR turns into the *unusual non-magnetic metallic* state. Because the PDOSs in the spin-up and spin-down channels of the edge Si atoms are below the Fermi level and do not cross the Fermi level, the edge Si is insulator state.

It should be mentioned that at $x = x_{down,h}$ hole doping, *N*-ZSiC NR starts to turn into the *unusual non-magnetic metallic* state, in which the edge C is in conduction, while the edge Si is in insulation. In contrast, at $x = x_{down,e}$ electron doping, *N*-ZSiC NR also starts to turn into *unusual non-magnetic metallic* state, but in which the edge Si is in conduction, while the edge C is in insulation. For comparison, Figure 6 shows the band structure and PDOS of the right and left edge C atoms in grapheme nanoribbon (4-ZCNR) for the electron doping $x = -0.60$ and hole doping $x = 0.70$. It is noted that when *N*-ZCNR is doped by a large amount of electron or hole, *N*-ZCNR turns into normal non-magnetic metallic state in which both C edges are in conduction. These can be understood as the following rationale. Both edges of *N*-ZGNR are terminated by the C atoms, and there is no electron transfer between both edges, hence no transverse charge polarization. As a result, both edge states of *N*-ZGNR are symmetric. However, in *N*-ZSiC NR, both edges are terminated by Si and C atoms, respectively. Due to the different electronegativity of Si and C atom, electron transfers from Si edge to C edge, hence Si and C atoms are charged positively and negatively, respectively. As a result, a transverse internal electric field appears across the ribbons.[48,49] Thus, both edge states of *N*-ZSiC NR are asymmetric. Note that, for both systems, the magnetic ground state as well as the characteristics of metallicity is determined by the band structures of the spin-up and spin-down at Fermi energy which originates from the edge states. Therefore, for *N*-ZSiC NR, electron doping carriers may enter the C edge state due to the transverse internal electric field, leading to the reduction in the local magnetic moment at the edge C. While hole doping carriers may enter the Si edge state, leading to the reduction in the local magnetic moment at the edge Si. However, for *N*-ZCNR, both the electron and hole doping carriers may enter both edge states, leading to the reduction in the local magnetic moment at both edge C.[57] Thus, when *N*-ZCNR is doped by a large amount of electron or hole, the local magnetic moment at both edge C disappears and *N*-ZCNR turns into normal non-magnetic metallic state in which both C edges are in conduction.

Conclusion

On the basis of systematic DFT calculations, it was found that the electron and hole doping effect are *asymmetry*, i.e, the electron critical doping value ($x_{down,e}$) is smaller than the hole critical doping value ($x_{down,h}$) and is almost independent of the width of *N*ZSiC NR though the other critical values of the electron and hole doping that influence the magnetization of *N*-ZSiC NR depend on the width. The most important finding is that at $x_{down,e}$ or $x_{down,h}$ doping, the *N*-ZSiC NR turns into *unusual non-magnetic metallic* state. The electron doping leads to the *N*-ZSiC NR's *unusual non-magnetic metallic* state, in which the edge Si is in conduction, while the edge C is in insulation. The hole doping also leads to *unusual non-magnetic metallic* state, in which the edge C is in conduction, while the edge Si is in insulation. To the best of our knowledge, such a *unusual non-magnetic metallic* state is reported for the first time, which shows a promising potential application in new generation of nano/molecular electronics and spintronics materials.

Acknowledgments. This work was supported by the National Natural Science Foundation of China (Grant No. 11174003) and the 211 Project of Anhui University. The work at SKKU was supported by the NRF Grant (No.2011-0001211) funded by the Korean Government (MEST). The

authors would like to acknowledge the support from KISTI supercomputing center through the strategic support program for the supercomputing application research [No. KSC-2011-C2-53].

References

1. Žutić, I., Fabian, J.; Das Sarma, S. *Rev. Mod. Phys*. **2004**, *76*, 323.
2. Kim, W. Y.; Kim, K. S. *Nature Nanotechnology* **2008**, *3*, 408.
3. Guo, J.; Gunlycke, D.; White, C. T. *Appl. Phys. Lett.* **2008**, *92*, 163109.
4. Muñoz-Rojas, F.; Fernández-Rossier, J.; Palacios, J. J. *Phys. Rev. Lett.* **2009**, *102*, 136810.
5. León, A.; Barticevic, Z.; Pacheco, M. *Appl. Phys. Lett.* **2009**, *94*, 173111.
6. Zheng, X. H.; Wang, R. N.; Song, L. L.; Dai, Z. X.; Wang, X. L.; Zeng, Z. *Appl. Phys. Lett.* **2009**, *95*, 123109.
7. Nguyen, V. H.; Do, V. N.; Bournel, A.; Nguyen, V. L.; Dollfus, P. *J. Appl. Phys.* **2009**, *106*, 053710.
8. Castro Neto, A.; Guinea, F.; Peres, N.; Novoselov, K.; Geim, A. *Rev. Mod. Phys*. **2009**, *81*, 109.
9. Han, M. Y.; Ozyilmaz, B.; Zhang, Y.; Kim, P. *Phys. Rev. Lett*. **2007**, *98*, 206805.
10. Berger, C.; Song, Z.; Li, X.; Wu, X.; Brown, N.; Naud, C.; Mayou, D.; Li, T.; Hass, J.; Marchenkov, A. N.; Conrad, E. H.; First, P. N.; Heer, W. A. D. *Science* **2006**, *312*, 1191.
11. Ci, L.; Xu, Z.; Wang, L.; Gao, W.; Ding, F.; Kelly, K.; Yakobson, B. I.; Ajayan, P. *Nano Res*. **2008**, *1*, 116.
12. Chen, Z.; Lin, Y.; Rooks, M. J.; Avouris, P. *Physica E* **2007**, *40*, 228.
13. Cancado, L. G.; Pimenta, M. A.; Neves, B. R. A.; Medeiros-Ribeiro, G.; Enoki, T.; Kobayashi, Y.; Takai, K.; Fukui, K.; Dresselhaus, M. S.; Saito, R.; Jorio, A. *Phys. Rev. Lett*. **2004**, *93*, 047403.
14. Lee, H.; Son, Y. W.; Park, N.; Han, S.; Yu, J. *Phys. Rev. B* **2005**, *72*, 174431.
15. Ezawa, M. *Phys. Rev. B* **2006**, *73*, 045432.
16. Son, Y. W.; Cohen, M. L; Louie, S. G. *Phys. Rev. Lett*. **2006**, *97*, 216803.
17. Ezawa, M. *Phys. Rev. B* **2007**, *76*, 245415.
18. Ezawa, M. *Physica E* **2008**, *40*, 1421.
19. Son, Y. W.; Cohen, M. L.; Louie, S. G. *Nature* (London) **2006**, *444*, 347.
20. Hod, O.; Barone, V.; Peralta, J. E.; Scueria, G. E. *Nano Lett*. **2007**, *7*, 2295.
21. Kan, E. J.; Li, Z.; Yang, J.; Hou, J. G. *Appl. Phys. Lett*. **2007**, *91*, 243116.
22. Hod, O.; Barone, V.; Scuseria, G. E. *Phys. Rev. B* **2008**, *77*, 035411.
23. Fujita, M.; Wakabayashi, K.; Nakada, K.; Kusakabe, K. *J. Phys. Soc. Jpn*. **1996**, *65*, 1920.
24. Wakabayashi, K.; Fujita, M.; Ajiki, H.; Sigrist, M. *Phys. Rev. B* **1999**, *59*, 8271.
25. Barone, V.; Hod, O.; Scuseria, G. E. *Nano Lett*. **2006**, *6*, 2748.
26. Kudin, K. N. *ACS Nano* **2008**, *2*, 516.
27. Sawada, K.; Ishii, F.; Saito, M. *Appl. Phys. Express* **2008**, *1*, 064004.
28. Sawada, K.; Ishii, F.; Saito, M.; Kawai, T. *Nano Lett*. **2009**, *9*, 269.
29. Sergio, D. D.; Zachary, H. L. *J. Phys. Chem. C* **2008**, *112*, 8196.
30. Zhang, X. W.; Yang, G. W. *J. Phys. Chem. C* **2009**, *113*, 4662.
31. Li, Y.; Zhou, Z.; Shen, P.; Chen, Z. *J. Phys. Chem. C* **2009**, *113*, 15043.
32. Sharma, R.; Nair, N.; Strano, M. S. *J. Phys. Chem. C* **2009**, *113*, 14771.
33. Lu, Y. H.; Feng, Y. P. *J. Phys. Chem. C* **2009**, *113*, 20841.
34. Li, Y.; Zhou, Z.; Shen, P.; Chen, Z. *ACS Nano* **2009**, *3*, 1952.
35. Nduwimana, A.; Wang, X. Q. *ACS Nano* **2009**, *3*, 1995.
36. Kinder, J. M.; Dorando, J. J.; Wang H.; Chan, G. K. L. *Nano Lett*. **2009**, *9*, 1980.
37. Hod, O.; Scuseria, G. E. *Nano Lett*. **2009**, *9*, 2619.
38. Biel, B.; Triozon, F.; Blase, X.; Roche, S. *Nano Lett*. **2009**, *9*, 2725.
39. Cantele, G.; Lee, Y. S.; Ninno, D.; Marzari, N. *Nano Lett*. **2009**, *9*, 3425.
40. Lee, H.; Ihm, J.; Cohen, M. L.; Louie, S. G. *Nano Lett*. **2010**, *10*, 793.
41. Kim, W. Y.; Kim, K. S. *Acc. Chem. Res*. **2010**, *43*, 111.
42. Wassmann, T.; Seitsonen, A. P.; Saitta, A. M.; Lazzeri, M.; Mauri, F. *J. Am. Chem. Soc*. **2010**, *132*, 3440.
43. Zheng, X. H.; Wang, X. L.; Abtew, T. A.; Zeng, Z. *J. Phys. Chem. C* **2010**, *114*, 4190.
44. Wu, M.; Wu, X.; Zeng, X. C. *J. Phys. Chem. C* **2010**, *114*, 3937.
45. Lee, Y. L.; Kim, S.; Park, C.; Ihm, J.; Son, Y. W. *ACS Nano* **2010**, *4*, 1345.
46. Lottermoser, T.; Lonkai, T.; Amann, U.; Hohlwein, D.; Ihringer, J.; Fiebig, M. *Nature* (London) **2004**, *430*, 541.
47. Eerenstein, W.; Wiora, M.; Prieto, J. L.; Mathur, N. D.; Scott, J. F. *Nature Mater*. **2007**, *6*, 348.
48. Lou, P.; Lee, J. Y. *J. Phys. Chem. C* **2009**, *113*, 21213.
49. Lou, P.; Lee, J. Y. *J. Phys. Chem. C* **2010**, *114*, 10947.
50. OpenMXWebsite. Ozaki, T.; Kino, H.; Yu, J.; Han, M. J.; Kobayashi, N.; Ohfuti, M.; Ishii, F.; Ohwaki, T.; Weng, H. http://www.openmx-square.org/.
51. Perdew, J. P.; Burke, K.; Ernzerhof, M. *Phys. Rev. Lett*. **1996**, *77*, 3865.
52. Troullier, N.; Martins, J. L. *Phys. Rev. B* **1991**, *43*, 1993.
53. Ozaki, T. *Phys. Rev. B* **2003**, *67*, 155108.
54. Ozaki, T.; Kino, H. *Phys. Rev. B* **2004**, *69*, 195113.
55. Lou, P.; Lee, J. Y. *J. Phys. Chem. C* **2009**, *113*, 12637.
56. Sun, L.; Li, Y.; Li, Z.; Li, Q.; Zhou, Z.; Chen, Z.; Yang, J.; Hou, J. G. *J. Chem. Phys*. **2008**, *129*, 174114.
57. Wu, F.; Kan, E.; Xiang, H.; Wei, S.; Whangbo, M.; Yang, J. *Appl. Phys. Lett*. **2009**, *94*, 223105.